

See discussions, stats, and author profiles for this publication at: <https://www.researchgate.net/publication/6653764>

# Lipid Profiling Reveals Arachidonate Deficiency in RAW264.7 Cells: Structural and Functional Implications †

ARTICLE *in* BIOCHEMISTRY · JANUARY 2007

Impact Factor: 3.02 · DOI: 10.1021/bi061723j · Source: PubMed

---

CITATIONS

39

---

READS

20

6 AUTHORS, INCLUDING:



[Pavlina Ivanova](#)

Vanderbilt University

54 PUBLICATIONS 1,681 CITATIONS

SEE PROFILE

Published in final edited form as:

*Biochemistry*. 2006 December 12; 45(49): 14795–14808.

## Lipid Profiling Reveals Arachidonate Deficiency in RAW264.7 Cells: Structural and Functional Implications†

Carol A. Rouzer<sup>‡,1</sup>, Pavlina T. Ivanova<sup>§,1</sup>, Mark O. Byrne<sup>§</sup>, Stephen B. Milne<sup>§</sup>, Lawrence J. Marnett<sup>‡,†</sup>, and H. Alex Brown<sup>§,†,\*</sup>

<sup>‡</sup>Department of Biochemistry, the Vanderbilt Institute of Chemical Biology, the Vanderbilt Ingram Cancer Center, Center in Molecular Toxicology, Center for Pharmacology and Drug Toxicology, Vanderbilt University School of Medicine, Nashville, TN 37232-0146 USA

<sup>§</sup>Department of Pharmacology, the Vanderbilt Institute of Chemical Biology, the Vanderbilt Ingram Cancer Center, Center in Molecular Toxicology, Center for Pharmacology and Drug Toxicology, Vanderbilt University School of Medicine, Nashville, TN 37232-0146 USA

<sup>†</sup>Department of Chemistry, the Vanderbilt Institute of Chemical Biology, the Vanderbilt Ingram Cancer Center, Center in Molecular Toxicology, Center for Pharmacology and Drug Toxicology, Vanderbilt University School of Medicine, Nashville, TN 37232-0146 USA

### Abstract

Glycerophospholipids containing arachidonic acid (20:4) serve as the precursors for an array of biologically active lipid mediators, most of which are produced by macrophages. We have applied mass spectrometry-based lipid profiling technology to evaluate the glycerophospholipid structure and composition of two macrophage populations, resident peritoneal macrophages and RAW264.7 cells, with regard to their potential for 20:4-based lipid mediator biosynthesis. Fatty acid analysis indicated that RAW264.7 cells were deficient in 20:4 ( $10 \pm 1$  mole percent) as compared to peritoneal macrophages ( $26 \pm 1$  mole percent). Mass spectrometry of total glycerophospholipids demonstrated a marked difference in the distribution of lipid species, including reduced levels of 20:4-containing lipids, in RAW264.7 cells as compared to peritoneal macrophages. Enrichment of RAW264.7 cells with 20:4 increased the fatty acid to  $20 \pm 1$  mole percent. However, the distribution of the incorporated 20:4 remained different from that of peritoneal macrophages. RAW264.7 cells pretreated with granulocyte-macrophage colony stimulating factor followed by lipopolysaccharide and interferon- $\gamma$  mobilized similar quantities of 20:4 and produced similar amounts of prostaglandins as peritoneal macrophages treated with LPS alone. LPS treatment resulted in detectable changes in specific 20:4-containing glycerophospholipids in peritoneal cells, but not in RAW264.7 cells. 20:4-enriched RAW264.7 cells lost 88% of the incorporated fatty acid during the LPS incubation without additional prostaglandin synthesis. These results illustrate that large differences in glycerophospholipid composition may exist, even in closely related cell populations, and demonstrate the importance of interpreting the potential for lipid-mediator biosynthesis in the context of overall glycerophospholipid composition.

Arachidonic acid (20:4)<sup>2</sup> and glycerophospholipids that contain 20:4 serve as the precursors for a broad array of potent, biologically active lipid mediators (prostaglandins (PGs), thromboxane, leukotrienes, lipoxins, hydroxyeicosatetraenoic acids, platelet activating factor, and endocannabinoids). In resting cells, 20:4 is predominantly found esterified in membrane

<sup>†</sup>This work was partially supported by LIPID MAPS U54 GM69338 (HAB) and GM15431 (LJM). HAB is an Ingram Associate Professor of Cancer Research in Pharmacology.

\*To whom correspondence should be addressed. Tel: (615) 936-3888. Fax: (615) 936-6833. alex.brown@vanderbilt.edu.

<sup>1</sup>CAR and PTI contributed equally to this work.

glycerophospholipids. Appropriate stimuli lead to the activation of cytosolic phospholipase A<sub>2</sub>, the enzyme primarily responsible for the selective hydrolysis of the ester bond linking 20:4 to the phospholipid glycerol backbone (1-4). Oxygenation of 20:4 by cyclooxygenase (prostaglandin endoperoxide synthase, COX) yields PGs, and thromboxane, while oxygenation by lipoxygenases yields leukotrienes, lipoxins, and hydroxyeicosatetraenoic acids (5-7). Platelet activating factor is generated from the lysolipid species formed by removal of 20:4 from a 1-alkyl-2-arachidonoylglycerophosphatidylcholine species (8). Alternative pathways lead to arachidonoyl ethanolamide and 2-arachidonoylglycerol, which comprise the endocannabinoids (9).

Macrophages are a major source of nearly all of the lipid mediators that are generated from 20:4-containing glycerophospholipids. These cells are capable of responding to a variety of stimuli with the biosynthesis of large quantities of PGs, leukotrienes, hydroxyeicosatetraenoic acids, and platelet activating factor (10-18). For example, Scott, et al. reported that in response to the phagocytosis of zymosan, murine resident peritoneal macrophages (RPM) mobilize as much as 50% of their glycerophospholipid 20:4, and convert nearly all of the released fatty acid to oxygenated products within a 2h period (10). 20:4 metabolism has been studied in numerous macrophage populations, including primary macrophages, and macrophage-like cell lines. It is well known that different macrophage populations deviate with regard to gene expression and response to stimuli, resulting in considerable variability in lipid mediator biosynthesis. However, little is known concerning the degree to which macrophage populations vary in glycerophospholipid structure and composition, or the degree to which such variation may contribute to differences in lipid mediator formation. Furthermore, although the biosynthetic pathways for lipid mediator biosynthesis have been well-defined at the level of the individual enzymes, relatively little is known concerning the effects that stimulus-dependent lipid mediator formation has on the structure and composition of the global glycerophospholipid metabolome.

The recent development of mass spectrometric (MS) techniques for the detection and analysis of total cellular lipids allows the detailed examination of the glycerophospholipid structure and composition of cells (19,20), providing an unprecedented opportunity to evaluate the comprehensive effects of cellular signaling events on the entire metabolome. Here we apply these techniques to a primary macrophage population, RPM, which has been extensively studied as a source of oxygenated 20:4 metabolites (10-16), and the RAW264.7 murine macrophage cell line (21), which is frequently used as a model for primary macrophages. The latter cells have been mainly studied with respect to alterations in the expression of genes relevant to the COX pathway (22-26). We report here that the steady state glycerophospholipid composition of RAW264.7 cells is markedly different from that of RPM, particularly with regard to the availability and distribution of the key fatty acid, 20:4. Furthermore, we demonstrate that bacterial lipopolysaccharide (LPS), under conditions leading to similar levels of 20:4 mobilization and PG biosynthesis, evokes distinct patterns of glycerophospholipid remodeling in the two cell populations. These results demonstrate the complexity of the sum total of all enzymatic activities that are modulated in response to a stimulus, and illustrate that highly divergent responses may be observed, even in closely related cell populations.

<sup>2</sup>Abbreviations: 20:4, arachidonic acid; PG, prostaglandin; COX, cyclooxygenase; RPM, resident peritoneal macrophages; MS, mass spectrometry; DMEM, Dulbecco's Modified Eagle Medium; FCS, fetal calf serum;  $\alpha$ -MEM, Minimum Essential Medium Alpha; LPS, lipopolysaccharide; IFN- $\gamma$ , interferon-gamma; GM-CSF, granulocyte-macrophage colony stimulating factor; BSA, bovine serum albumin; PBS, calcium- and magnesium-free phosphate-buffered saline; SFM-20:4, Macrophage Serum-Free Medium containing arachidonic acid-bovine serum albumin complexes; GPCho, phosphatidylcholine; GPEtn, phosphatidylethanolamine; GPIIns, phosphatidylinositol; GPSer, phosphatidylserine; GPGro, phosphatidylglycerol

## Experimental Procedures

### RAW264.7 Cell Cultures

RAW264.7 cells were obtained from the American Type Culture Collection. The cells were maintained in Dulbecco's Modified Eagle Medium supplemented with GlutaMax, high glucose, sodium pyruvate, and pyridoxine-HCl (Gibco, Grand Island, NY) containing 10% heat inactivated fetal calf serum (Atlas Biologicals, Norcross, GA) (DMEM/FCS). Cells were plated onto 35 mm tissue culture dishes at  $5 \times 10^5$  cells/dish (for PG analysis) or onto 60 mm dishes at  $1.5 \times 10^6$  cells/dish (for glycerophospholipid and fatty acid analysis) on the day prior to experiments. For most experiments, medium was changed to DMEM/FCS containing 20 ng/ml GM-CSF (R&D Systems, Minneapolis, MN) 2 h after plating, and cells were incubated overnight (20 - 22 h total).

### Enrichment of RAW264.7 Cells with 20:4

A solution (0.25 ml) of 20 mg/ml 20:4 (NuChek Prep, Elysian, MN) in chloroform was placed in an acid-washed glass tube and the solvent was evaporated to dryness under argon. KOH (1.25 ml of a 0.015 M solution) was added to the resulting film. The tube was sealed under argon and incubated at 37°C for 1 h. Fatty acid- and endotoxin-free bovine serum albumin (BSA, 1.25 g, Sigma) was dissolved in 40 ml of calcium- and magnesium-free phosphate-buffered saline (PBS), and added to the tube, which was sealed under argon and incubated at 37°C with agitation for 24 h. The pH of the solution was corrected to 7.4, and PBS was added to a final volume of 50 ml. The resulting solution was stored under argon at -20°C. On the day of the experiment, the solution was thawed and diluted 1:10 in Macrophage Serum-Free Medium (Gibco) to give a final BSA concentration of 2.5 mg/ml and a final 20:4 concentration of 10 µg/ml (SFM-20:4). The medium was filtered, and 20 ng/ml of GM-CSF was added. This medium was used instead of DMEM/FCS plus GM-CSF during the 20 - 22 h incubation period prior to addition of stimuli (27,28).

### RPM Culture

All studies involving animals were done with the approval of the Institutional Animal Care and Use Committee of Vanderbilt University. Female ICR (CD-1) mice (25-30g) were obtained from Harlan (Indianapolis, IN). Cells were obtained by peritoneal lavage as described previously (29) and suspended at 2 to  $3 \times 10^6$  cells/ml (cells from one mouse/2 ml) in Minimal Essential Medium Alpha supplemented with GlutaMax (Gibco), containing 10% heat inactivated serum plus 100 Units/ml penicillin and 0.10 mg/ml streptomycin (Sigma, St. Louis, MO) ( $\alpha$ -MEM/FCS). The cell suspension was plated onto 60 mm dishes at 6 ml per dish and incubated for 2 hours at 37°C in a humidified 5% CO<sub>2</sub> atmosphere. Nonadherent cells were removed by washing the plates four times with PBS, and the cultures were then incubated overnight in fresh  $\alpha$ -MEM/FCS.

### Treatment of RAW264.7 or RPM Cultures with Stimuli

Cells were plated in 35 mm or 60 mm dishes and incubated overnight as described above. RAW264.7 cells were then transferred to fresh DMEM/FCS with or without LPS (100 ng/ml, *E. coli* 011:B4, Calbiochem, San Diego, CA) and/or murine recombinant IFN- $\gamma$  (10 ng/ml, Sigma) as desired. GM-CSF (20 ng/ml) was also included in the medium of cells that had been preincubated overnight with that cytokine. RPM were washed twice in PBS and transferred to fresh  $\alpha$ -MEM/FCS with or without LPS (100 ng/ml). Cultures were incubated for the desired time periods. Medium was then harvested for analysis of PG formation, and cells were scraped for lipid or protein analyses as described below.

## Assay of PGs

Following incubation with desired stimuli, the medium was removed from cultures (35 mm dishes), placed on ice, and immediately spiked with 20  $\mu$ l of a methanol solution containing 50 pmol each of PGE<sub>2</sub>-d<sub>4</sub> and PGD<sub>2</sub>-d<sub>4</sub> (Cayman Chemical, Ann Arbor, MI), which served as internal standards. Samples were stored at -20°C prior to solid phase extraction and analysis by selected reaction monitoring of the ammoniated ions by liquid chromatography positive ion electrospray ionization tandem mass spectrometry (LC-MS/MS) as described (30). The major PGs produced by RAW264.7 cells are PGD<sub>2</sub> and PGE<sub>2</sub>, which are formed at a ratio of approximately 4 to 1. Values for PG formation are the sum of these two products. Data were normalized to the protein content of the cell monolayers (determined using a BCA Protein Assay kit, Pierce, Rockford, IL) and then to cell number based on a conversion factor of 1.27 mg cell protein/10<sup>7</sup> cells.

## Phospholipid Fatty Acid Analysis

Cells in 60 mm culture dishes were scraped twice into a total volume of 1.0 mL of PBS. The cells from two dishes were combined, recovered by centrifugation at 750  $\times$  g for 5 min, and resuspended in 0.5 mL of PBS. The resulting cell suspensions were stored at -80°C until analysis by gas chromatography by the Vanderbilt University Mouse Metabolic Phenotyping Center laboratory (31).

## Total Cell Glycerophospholipid Analysis

After incubation with desired stimuli, plates were placed on ice and washed with 1.5 ml of ice-cold PBS. Cell extracts were prepared via a modified Bligh/Dyer extraction procedure (32). Briefly, cells were scraped into 800  $\mu$ l of 0.1 N HCl:CH<sub>3</sub>OH (1:1) and 400  $\mu$ l CHCl<sub>3</sub> was added to the suspension. The samples were vortexed for 1 min and layers were separated by centrifugation at 18 000  $\times$  g for 5 min at 4°C. The organic phase was isolated and the solvent was evaporated in a vacuum centrifuge (Labconco Centrивap Concentrator, Kansas City, MO). Samples were redissolved in 70  $\mu$ l of CH<sub>3</sub>OH:CHCl<sub>3</sub> (9:1) and 1  $\mu$ l of concentrated (18 M) aqueous NH<sub>4</sub>OH was added before analysis. Mass spectral analysis was performed on a Finnigan TSQ Quantum triple quadrupole mass spectrometer (ThermoFinnigan, San Jose, CA) equipped with a Harvard Apparatus syringe pump and an electrospray source. Samples were analyzed at an infusion rate of 10  $\mu$ l/min in both positive and negative ionization modes over the range of  $m/z$  350 to 1200. Data were collected with the Xcalibur software package (ThermoFinnigan) and analyzed with software developed in our laboratory. Identification of individual glycerophospholipids was accomplished by tandem mass spectrometry (ESI-MS/MS) (33).

## Data Analysis

Each MS sample file consisted of approximately 60 scans (instrument sweeps of 1 per second for 60 seconds) each of which had 11,428 unique  $m/z$  values at a resolution of 0.07 amu. The MS scans (.Raw files) were batch converted to a non-proprietary ascii compatible form using the vendor supplied Windows32 executable Xconvert.exe. The ascii files were parsed, filtered for anomalous scans, and time-averaged. A peak finding algorithm was applied to the time-averaged array. The maximum ion intensity value on 1 amu intervals was used to determine the peak maximum intensity and the associated nominal  $m/z$  and peak maximum were written to a file. Files were batch processed using a Windows executable generated in Fortran G77 (GNU) (Byrne, M.O. and Brown, H.A. unpublished data). Comparative statistical analysis (unpaired t-tests) and normalization of peak data were performed in S-Plus<sup>®</sup> Version 3.3 for Windows software suite (MathSoft, Inc. Cambridge, MA).

## Immunoblotting for Protein Expression

For the determination of the expression of the inducible isoform of COX (COX-2), cell monolayers were washed twice with ice cold PBS and scraped twice into a total volume of 200  $\mu$ l of lysis buffer (50 mM Tris-HCl, pH 7.5, plus 150 mM NaCl, 4 mM EDTA, 50 mM NaF, 0.1 mM  $\text{Na}_3\text{VO}_4$ , 0.2% Triton X-100, 0.1% NP40, 0.5% sodium deoxycholate, 1 mM dithiothreitol, 1 mg/ml AEBSF, and 5  $\mu$ g/ml each of antipain, leupeptin, chymostatin, and pepstatin (all components from Sigma)). Cell lysates were stored at  $-80^\circ\text{C}$  prior to analysis by immunoblot as described (29,34). A chemiluminescence signal was generated with ECL detection reagent (Amersham, GE Healthcare Biosciences, Piscataway, NJ), and the signal intensity was measured using a Fluor-S Max Multi-Imager (BioRad, Hercules, CA).

## Results

### Phospholipid Fatty Acid Composition of RAW264.7 Cells Versus RPM

Glycerophospholipid structure is strongly dependent upon the component fatty acids. Consequently, we initially evaluated the phospholipid fatty acid composition of the RAW264.7 cells and RPM. RAW264.7 cells were plated and preincubated for 22 h in DMEM/FCS containing GM-CSF, whereas RPM were isolated and incubated overnight in  $\alpha$ -MEM/FCS. The cells were then harvested for phospholipid fatty acid analysis. GM-CSF pretreatment of RAW264.7 cells was used for these studies, because, as described below, it facilitates lipid mediator synthesis in those cells. This pretreatment was exhaustively examined, and was found to have no effect on phospholipid fatty acid composition, or on glycerophospholipid species distribution (data not shown). The phospholipid fatty acid compositions of RAW264.7 cells and RPM are shown in Table 1. (The fatty acids are designated by two numbers, xx:y, where xx is the total number of carbon atoms, and y is the number of double bonds). The two cell populations differed considerably, particularly with regard to the content of 20:4, which was  $26 \pm 1$  mole% in RPM as compared to  $10 \pm 1$  mole% in RAW264.7 cells. The deficit in 20:4 was compensated in RAW264.7 cells primarily by increased levels of oleate (18:1,  $32 \pm 1$  mole % in RAW264.7 cells versus  $7.8 \pm 0.3$  mole% in RPM), and to a lesser degree, palmitoleate (16:1). Also notable was the increased levels of 22-carbon polyunsaturated fatty acids (22:4, 22:5, and 22:6) in RPM as compared to RAW (Table 1).

An obvious possible explanation for the low 20:4 content of RAW264.7 cells as compared to RPM is that RAW264.7 cells are maintained in FCS-containing culture medium, which is an inadequate source of 20:4, whereas RPMs, reflect the nutrients available in vivo. In order to test this hypothesis, we attempted to increase the phospholipid 20:4 content by incubating RAW264.7 cells for 22 h in serum-free medium containing a preformed 20:4-BSA complex (SFM-20:4) (27,28). Since this treatment replaced the preincubation period with GM-CSF, the cytokine was also included in the medium. As indicated in Table 1, the 20:4 enrichment protocol resulted in a two-fold increase in the phospholipid 20:4 content of the cells. Also observed was a large increase in docosatetraenoic acid (22:4), resulting from chain elongation of the added 20:4. These increases in polyunsaturated fatty acids were counterbalanced by decreases primarily in stearate (18:0) and oleate (18:1).

### Identification of Glycerophospholipid Species in Macrophage Populations

The marked differences in phospholipid fatty acid composition between RPM and RAW264.7 cells implied that the two cell populations must differ in the relative distribution of individual species within each of the major glycerophospholipid classes. This hypothesis was tested by MS and MS/MS analysis of the total glycerophospholipids in RAW264.7 cells, in RAW264.7 cells following 20:4 enrichment, and in RPM following isolation and overnight incubation. We have extensively characterized the individual glycerophospholipid species found in RAW264.7 cells. Species identities for the five major glycerophospholipid classes,



phosphatidylcholine (GPCho), phosphatidylethanolamine (GPEtn), phosphatidylinositol (GPIIns), phosphatidylserine (GPSer), and phosphatidylglycerol (GPGro) are summarized in Supplemental Information (Table 1 Supplement). Since these data were acquired from both resting cells, and cells exposed to various stimuli, they represent species that might be found in RAW264.7 cells (RAW) under a variety of conditions. Similar data have also been acquired for RPM and for RAW264.7 cells enriched with 20:4 (EN-RAW) however, these cell populations have not been as thoroughly studied. Consequently, the absence of a species that has been identified in RAW264.7 cells from RPM or 20:4-enriched RAW264.7 cells does not necessarily mean that this species does not occur in the latter two cell types. Note that Table 1 Supplement designates each species by a number,  $xx:y$ , where  $xx$  is the total number of carbons and  $y$  is the total number of double bonds in the two fatty acyl chains. A designation of “ $e$ ” indicates that the fatty acid at the  $sn-1$  position is ether-linked, while the “ $p$ ” designation indicates a vinyl ether linkage (35). For reference, Table 2 summarizes phospholipid structure and the nomenclature used here. Table 1 Supplement highlights similarities and differences between the macrophage populations. For a given species, multiple combinations of fatty acids might be possible. Table 1 Supplement provides data for all combinations that have been identified by fragmentation MS/MS analysis.

Subtle differences were noted in the species identified in RPM as compared to RAW264.7 cells. In most cases, these differences could be explained on the basis of a higher content of 20:4 and polyunsaturated 22-carbon fatty acids in RPM. For example, RPM contained GPGro species including 38:5, 42:10, 42:9, and 42:8 all of which contained 20:4. The latter three species also contained 22:4, 22:5, or 22:6. None of these species was detected in RAW264.7 cells, but all three were detected in 20:4-enriched RAW264.7 cells, as might be expected to result from the increased content of 20:4 and 22:4 in those cells.

### Total Glycerophospholipid Composition of RAW264.7 Cells Versus RPM

Analysis of the total glycerophospholipid composition for resting RPM, RAW264.7 cells, and 20:4-enriched RAW264.7 cells was performed separately for each of the five major classes. The analysis was limited to species that had been positively identified in at least one of the cell types. For each glycerophospholipid class, the total of the mass spectral peak (signal) intensities from all species in that class was determined, and the signal from each species was calculated as the percent of that total. It should be noted that mass spectral signal intensity decreases with increasing chain length and degree of unsaturation of the component fatty acids (36), so these relative signal intensity data are not a direct assessment of absolute quantity. However, comparisons of these relative signal patterns do allow an assessment of differences in the distribution of individual species within a class, which are readily apparent in an evaluation of the data from RAW264.7 cells and RPM.

For an initial comparison, the percent signal intensities of all 20:4-containing species for lipids in each class were summed. (These species were identified using Table 1 Supplement). The results are shown in Table 3. It is immediately apparent that 20:4-containing species comprise a higher percent of each glycerophospholipid class in RPM than in RAW264.7 cells. The most striking difference is seen in GPCho, for which the relative signal intensities of 20:4-containing lipids in RAW264.7 cells ( $19 \pm 3\%$ ) were considerably weaker than those observed in RPM ( $48 \pm 1\%$ ). In contrast, for GPEtn, the relative signal intensities of 20:4-containing lipids more closely resembled those in RPM, and for GPSer, they were nearly equal. Using absolute quantities of each glycerophospholipid class in RPM (169 nmol/mg protein (28)) and RAW264.7 cells (145 nmol/mg protein (37)), along with our measured value for the protein content ( $1.27 \text{ mg}/10^7 \text{ cells}$ ) of RAW264.7 cells the percent signal intensities in Table 3 were converted to estimated absolute quantities (in nmol/ $10^7 \text{ cells}$ ). These values are given in Table 3 in parentheses. These estimates are subject to two major sources of error, the differences in

ionization efficiency mentioned above, and the fact that most mass spectrometry signals originated from a mixture of lipids made up of varying fatty acyl compositions (Table 1 Supplement). In calculating the percentages in Table 3, the entire signal was assumed to be attributable to a 20:4-containing lipid. The first source of error will lead to an underestimation of 20:4-containing lipids, as long chain polyunsaturated fatty acids such as 20:4 have a relatively poor ionization efficiency. The second source of error will lead to an overestimation of 20:4-containing lipids, because signal intensity from lipids that do not contain 20:4 were included in the calculation. Despite these potential errors, the calculation provides some useful information, because it allows a rough comparison of the amount of 20:4 containing lipids across lipid classes. These results suggest that both GPCho and GPEtn may serve as major sources of 20:4 in RPM and RAW264.7 cells.

The differences in glycerophospholipid 20:4 content between RPM and RAW264.7 cells also affected the relative distribution of 20:4 among lipid species within each class. Figs. 1A through 5A show a direct comparison of the relative signal intensity data for the 10 species showing the largest differences in RAW264.7 cells versus RPM for GPCho, GPEtn, GPIIns, GPSer, and GPGro, respectively. The differences were statistically significant ( $p < 0.05$ ) for all species except where indicated by an asterisk. These figures highlight the limited number of species that showed marked differences between the cell types, while a general similarity in distribution for the majority of the lipids is illustrated in Figs. S1A through S5A (Supplemental Material), which show the results for all species analyzed. It is immediately evident from Figs. 1A through 5A that RPM lipids contained a much higher percentage of select species that incorporated 20:4 (notably in GPCho, GPEtn, and GPIIns) and other long-chain polyunsaturated fatty acids (notably in GPSer and GPGro). In RAW264.7 cells, glycerophospholipids containing 18:0, 18:1, 16:0, and 16:1 were generally more prominent. In particular, it is notable that for GPCho, RPM contained much higher levels of the diacyl 38:4 and 36:4 GPCho species as well as the corresponding alkyl acyl species, whereas for GPEtn, 20:4-containing alkyl acyl species (38:4p/38:5e and 36:4p GPEtn) were particularly prominent as compared to RAW264.7 cells. For GPIIns, RPM were notable for their relative enrichment of 38:4 and 38:4p/38:5e/37:4 GPIIns. While 38:4 GPSer is the predominant GPSer species in RPM, these cells also contained relatively more 40:1, 40:2, and 40:4 GPSer than did RAW264.7 cells. In contrast, 36:1 GPSer was clearly prominent in the latter cell population. GPGro appeared to be a repository for long-chain polyunsaturated fatty acids in RPM, whereas RAW264.7 cells contained predominantly 36:2 and 34:1 GPGro, reflecting the relatively high 18:1 enrichment in those cells.

### Effect of 20:4 Enrichment on RAW264.7 Cell Glycerophospholipids

As noted above, incubation of RAW264.7 cells in SFM-20:4 caused an enrichment of phospholipid 20:4 to levels similar to those found in RPM. The 22 h incubation period was chosen, because it had been previously shown that exogenously supplied 20:4 is initially found predominantly in GPCho and over time is redistributed to GPEtn and GPIIns (38). Thus, the intent of the extended incubation was to provide adequate time for the 20:4 to reach a steady state distribution throughout the various glycerophospholipid pools. As seen in Table 3, this supplementation resulted in an increase in 20:4-containing lipid species in all glycerophospholipid classes, except GPSer, with the largest increases observed in GPCho and GPGro. As a result, the percent of signal intensity values corresponding to 20:4-containing lipids in 20:4-enriched RAW264.7 cells more closely resembled the values observed in RPM, and for GPGro the value exceeded that in RPM.

The effect of 20:4 enrichment on the distribution of distinct species within each of the major classes was evaluated using MS. Figs. 1B through 5B show a direct comparison of the relative signal intensity data in unenriched versus 20:4-enriched RAW264.7 cells for GPCho, GPEtn, GPIIns, GPSer, and GPGro, respectively. These figures highlight the few species that were



markedly different between the cell populations, while Figs. S1B through S5B (Supplemental Material) provide data for all species analyzed. For GPCho and GPIs, the species showing the largest relative increases were the 20:4-containing 36:4 and 38:5 GPCho/GPIs. These were offset predominantly by decreases in lipids containing 16:0, 16:1, 18:0, and 18:1. In all other classes, the largest relative increases were observed in species that contained over 40 carbons total, representing combinations of 20:4 or 22:4 with 18-carbon, or other 20-carbon fatty acids.

20:4 enrichment did not result in a phospholipid distribution pattern in RAW264.7 cells that closely resembled that of RPM, as illustrated in Figs. 1C through 5C, which summarize data for the species that showed the largest differences between the cell types. Data for all species are provided in Figs. S1C through S5C in Supplemental Material. These data demonstrate that, even though the overall proportion of 20:4-containing lipids increased with enrichment in RAW264.7 cells, the 20:4 had been incorporated into different species from those found in RPM. For example, in RPM, the predominant 20:4-containing GPCho was 38:4 GPCho, whereas in enriched RAW264.7 cells, it was 36:4 GPCho. Enriched RAW264.7 cells contained relatively more 38:5 GPCho than did RPM. For GPEtn, 20:4 enrichment led to increases in 38:4 GPEtn and 36:4 GPEtn, but in RPM, alkyl acyl GPEtns were the predominant 20:4-containing species. 20:4 enrichment led to a large increase in 40:8 GPGro in RAW264.7 cells, whereas this was not one of the main long-chain polyunsaturated GPGro species in RPM. Thus, it is clear that although 20:4 enrichment resulted in a major remodeling of RAW264.7 cell phospholipids, the resulting distribution did not resemble that in RPM, at least not within a 22 h incubation period.

### LPS-Dependent PG Synthesis in RAW264.7 Cells

The relative deficiency of 20:4 in RAW264.7 cells as compared to RPM might be expected to lead to reduced lipid mediator biosynthesis in these cells. Indeed, prior studies have shown that RAW264.7 cells produce lower quantities of PGs than RPM in response to 100 ng/ml of LPS ( $1,900 \pm 200$  versus  $6,900 \pm 1,400$  pmol/ $10^7$  cells, respectively) (34,39). However, it is equally likely that the reduced PG synthesis in RAW264.7 cells is due to a poor ability to respond to the LPS stimulus, resulting from lower levels of expression of the relevant enzymes and/or receptor-linked stimulus response coupling mechanisms. GM-CSF and IFN- $\gamma$ , are cytokines that have been shown to augment cellular responses to LPS (40-42). As shown in Fig. 6, preincubation of RAW264.7 cells for 20 - 22 h with 20 ng/ml of GM-CSF effected a 2.6-fold increase in PG synthesis in response to LPS alone. Incubation with IFN- $\gamma$  (10 ng/ml) induced no significant PG formation, whether or not cells had been pretreated with GM-CSF. However, inclusion of IFN- $\gamma$  with LPS resulted in a 1.3-fold further increase in PG formation, resulting in the accumulation of  $6,400 \pm 1,400$  pmol/ $10^7$  cells in the case of cells preincubated with GM-CSF. These results clearly demonstrated that GM-CSF pretreatment and IFN- $\gamma$  cotreatment could significantly augment the capacity of these cells for PG biosynthesis, resulting in levels similar to those obtained in RPM stimulated with LPS alone. Consequently, it is evident that the deficiency of phospholipid 20:4 in RAW264.7 cells relative to RPM does not necessarily lead to lower levels of PG formation.

### Effect of LPS on RPM and RAW264.7 Cell Glycerophospholipids

The formation of 6 to 7 nmol of PGs/ $10^7$  cells in response to LPS requires a substantial mobilization of 20:4 from glycerophospholipids, and must result in significant lipid remodeling. In order to evaluate the effects of LPS-dependent PG synthesis on glycerophospholipids, RAW264.7 cells were plated and preincubated for 22 h with GM-CSF, followed by 5 h with LPS/IFN- $\gamma$ . RPM were isolated, incubated overnight, and then treated for 5 h with LPS alone. At the end of the 5 h LPS incubation periods, cells were collected and

subjected to phospholipid fatty acid analysis and MS analysis of total cell glycerophospholipids.

As shown in Table 1, LPS treatment resulted in a decrease in phospholipid 20:4 content in both RPM and RAW264.7 cells. Using the published value for the phospholipid content of RPM (28) and RAW264.7 cells (37), the mole fraction data were converted to an estimated absolute quantity of 20:4 for control and LPS-treated cells. These results were then used to determine the amount of 20:4 mobilized and then lost from phospholipid as a result of the LPS stimulation. As seen in Table 4, LPS caused a similar mobilization of 20:4 from RAW264.7 cells and RPM, even though the amount mobilized represented a greater fraction of phospholipid 20:4 (29%) in the RAW264.7 cells as compared to RPM (9%).

Figs. 7A through 11A show a direct comparison of the relative signal intensity data in unenriched control versus unenriched LPS/IFN- $\gamma$ -treated RAW264.7 cells for GPCho, GPEtn, GPIIns, GPSer, and GPGro, respectively. Comparable data are found for 20:4-enriched RAW 264.7 cells in Figs. 7B through 11B, and for RPM in 7C through 11C. In each case, the figures show results for the 10 species that showed the greatest changes in response to LPS. Species for which the changes were statistically significant ( $p < 0.05$ ) are indicated by a star. Data for all species analyzed are found in Figs. 7S through 11S in Supplemental Material. The RAW264.7 cell data show very little difference in the relative distribution of phospholipids as a result of the LPS/IFN- $\gamma$  treatment. In fact, the only changes in 20:4-containing lipids that were statistically significant ( $p < 0.05$ ) were for 40:4 and 40:5 GPIIns, and 38:4 GPSer. A rather large decrease in 38:4 GPIIns was not significant, due to considerable variability in the relative levels of this lipid in control cells. In contrast, RPM lipids showed substantial and significant decreases in the 20:4-containing 38:4, 38:4p/38:5e, 36:4, and 36:4e GPCho, 36:4p GPEtn, and 38:4 GPIIns.

### Effect of LPS/IFN- $\gamma$ Treatment on 20:4-Enriched RAW264.7 Cell Lipids

As shown in Tables 1 and 4, when 20:4-enriched RAW264.7 cells were treated with LPS/IFN- $\gamma$  for 5 h, they exhibited a 43% loss of phospholipid 20:4, a 3-fold increase over the quantity lost by unenriched RAW264.7 cells or RPM. In contrast the elevated levels of 22:4 that resulted from enrichment did not change. The higher level of 20:4 mobilization in the enriched cells could either be due to greater utilization of substrate for lipid mediator biosynthesis, or to exchange with serum proteins in the medium, as was previously described for 18:0-enriched RPM (27,28). As seen in Fig. 12A, enriched RAW264.7 cells produced the same quantities of PGs as did unenriched cells. This finding suggests that PG synthesis is limited by the levels of available enzymes, consistent with the finding that induction of COX-2 protein expression was the same in the enriched and unenriched cells (Fig 12B). This result does not support the hypothesis that the greater level of 20:4 mobilized in 20:4-enriched RAW264.7 cells as compared to unenriched cells was utilized for lipid mediator synthesis. Alternatively, it is possible that 20:4 is simply being exchanged with serum proteins, a process that might render it unavailable for oxygenation by COX. This hypothesis is supported by the data in Figs. 7B through 11B. These data demonstrate that the species that show the greatest decrease during the LPS/IFN- $\gamma$  incubation are in most cases the same species that showed the greatest increase with 20:4 enrichment (Figs. 1B through 5B). This is particularly striking in the case of GPCho, for which 8 of the 10 species that showed the greatest increases with enrichment also showed the greatest decreases with LPS/IFN- $\gamma$  incubation. Thus, it appears that the changes occurring during the LPS incubation period primarily reflect a reversal of the enrichment process rather than a selective mobilization of 20:4 for lipid mediator synthesis.

## Discussion

The availability of new MS-based lipid profiling techniques provides, for the first time, a comprehensive and contextual evaluation of steady state glycerophospholipid composition and global changes in that composition as a function of defined cell signaling and metabolic perturbations. Here we apply this technology to demonstrate that RAW264.7 cells are strikingly different from RPM in phospholipid fatty acid content and in the distribution of fatty acids among glycerophospholipid species. The predominant difference is the markedly lower 20:4 content, leading to a reduction in the levels of selected 20:4-containing species in RAW264.7 cells as compared to RPM. Based on the relative signal intensity data for each lipid class (Table 3) it appears that the deficit of 20:4-containing species in RAW264.7 cells is greater for GPCho than for GPEtn. However, conversion of the signal intensity data to estimated absolute quantities, which takes into account the differences in the proportions of GPCho and GPEtn between RPM and RAW264.7 cells, leads to the conclusion that the absolute amount of 20:4 in the two major phospholipid classes is roughly equal in both cell types, and that the deficit in RAW264.7 cells compared to RPM is also similar for the two lipid classes (Table 3). As noted previously, the use of signal intensity data to estimate absolute quantities of lipids is subject to significant sources of error; however, it is notable that the total amount of 20:4-containing lipids estimated from signal intensity data for each cell type in Table 3 (110 nmol/10<sup>7</sup> cells for RPM, 44 nmol/10<sup>7</sup> cells for RAW264.7 cells, and 76 pmol/10<sup>7</sup> cells for 20:4-enriched RAW264.7 cells) agrees remarkably well with the estimated 20:4 content obtained from fatty acid analysis data, which are not subject to the same error source (Table 4). Nevertheless, the conclusion that 20:4 is approximately equally distributed between GPCho and GPEtn contrasts with previous reports indicating that GPEtn is the predominant source of 20:4 in the J774 macrophage cell line and polymorphonuclear leukocytes (38,43). Further studies, including absolute quantification of lipid species, will be required to verify the exact distribution of 20:4 in the lipids of RPM and RAW264.7 cells.

The much lower level of 20:4 in RAW264.7 cells as compared to RPM could be due to multiple factors. First, the long-term maintenance of cells in culture medium containing FCS, which is not a major source of 20:4, could eventually lead to a loss of this fatty acid. Second, RAW264.7 cells were originally derived from pristane-elicited peritoneal cells, which may exhibit fundamentally different lipid metabolism from RPM, and finally, metabolic changes may have resulted from the process of Abelson leukemia virus transformation during the generation of the RAW264.7 cell line (21). Our data support the hypothesis that there are basic differences in lipid metabolic pathways between RAW264.7 cells and RPM that are not readily explained by the availability of fatty acids in the culture medium. This is illustrated by the fact that RAW264.7 cells and RPM demonstrate fundamental differences in the distribution of fatty acids among their phospholipids. Upon 20:4 enrichment of RAW264.7 cells, the incorporated fatty acid is found in distinctly different glycerophospholipid species than in RPM, even after allowing 22 h for the fatty acid to equilibrate with the existing lipid pools. 20:4-enriched RAW264.7 cells rapidly mobilize 43% of their phospholipid 20:4 (corresponding to 88% of the fatty acid incorporated during enrichment) as a result of incubation with LPS/IFN- $\gamma$  in serum-containing medium. In contrast, RPM maintain high phospholipid 20:4 content after isolation and overnight incubation in serum-containing medium. Incubation of these cells with LPS in the presence of serum mobilized only 9% of their 20:4. Furthermore, when RPM are enriched with 18:0, and then transferred to serum-containing medium, a rapid efflux of the incorporated saturated fatty acid is observed (27,28). Together, these observations suggest that RPM incorporate 20:4 into highly stable metabolic pools, and/or that they possess enzymes that selectively scavenge and retain 20:4. These pathways appear to be deficient in RAW264.7 cells.

An additional striking difference in 20:4 distribution between RPM and RAW264.7 cells lies in the much higher content of lipids containing ether and vinyl ether linkages at the *sn-1* position. This is particularly notable for GPEtn, where 38:4p/38:5e and 36:4p species predominate in RPM, but are relatively minor species in RAW264.7 cells. 20:4 enrichment does not result in a proportionate increase in these species in RAW264.7 cells, suggesting a relative deficiency in alkyl acyl and alkenyl acyl lipid synthesis in those cells, as compared to RPM. This finding is significant in view of the previously reported role of these species as a source of 20:4 in stimulus-dependent lipid remodeling in polymorphonuclear leukocytes and macrophages (44,45). Furthermore, since 1-alkyl-2-arachidonoyl GPCCho species are the precursors of platelet activating factor, the relative deficiency of these species in RAW264.7 cells may have an impact on the biosynthesis of this lipid mediator (8).

The lower phospholipid 20:4 content in RAW264.7 cells as compared to RPM might be expected to result in reduced synthesis of other lipid mediators that are formed directly from 20:4. We tested this hypothesis with regard to LPS-dependent PG synthesis, which we had previously reported to be lower in RAW264.7 cells than in RPM. However, GM-CSF pretreatment significantly augmented LPS-dependent PG formation in RAW264.7 cells without altering glycerophospholipid fatty acid composition or species distribution. Furthermore, when RAW264.7 cells were pretreated with GM-CSF and co-treated with INF- $\gamma$ , they produced PGs at similar levels as those produced by RPM treated with LPS alone. These data demonstrate that RAW264.7 cells require additional stimulation in order to be able to respond to LPS to the same degree as RPM, but if so treated, they can produce PGs in the same quantities as RPM despite their lower levels of glycerophospholipid 20:4. Further evidence that PG synthesis is not primarily dictated by the level of 20:4 in glycerophospholipids was provided by the finding that 20:4-enriched RAW264.7 cells produce no additional PGs, despite markedly increased 20:4 mobilization. Note, however, that in the case of unenriched RAW264.7 cells, the production of large quantities of PGs in response to LPS renders the cell phospholipids even more deficient in 20:4 as compared to LPS-treated RPM. This may reduce their ability to respond to a secondary stimulus, such as zymosan phagocytosis, with PG formation.

Despite the fact that LPS/INF- $\gamma$  treatment of GM-CSF pretreated RAW264.7 cells evoked mobilization of similar amounts of 20:4 as did LPS treatment of RPM, the two cell types differed with regard to observed changes in species distribution in glycerophospholipid classes. Few significant changes were noted in glycerophospholipids as a result of LPS/INF- $\gamma$  treatment of RAW264.7 cells, whereas RPM exhibited decreases in 20:4-containing GPCCho, GPEtn, and GPIIns species. This finding might reflect a higher degree of specificity for mobilization of 20:4 from selected lipid species in RPM, making it easier to detect changes in those species. It is notable, however, that the level of variability between experiments was greater for RAW264.7 cells than for RPM, rendering it more difficult to achieve statistical significance in changes that were observed, such as in 38:4 GPIIns (Fig. 10A). It should also be noted that these studies were carried out at a single 5 h time point, and therefore identify pools of lipids that ultimately served as a source of 20:4. They do not address the possibility that other lipids were initially used to provide 20:4 for PG synthesis, and were then replenished from the stores that we have identified. Full time course studies will be required to address the possibility of dynamic lipid fluxes.

It is clear from the phospholipid fatty acid compositions of RAW264.7 cells and RPM that a major difference exists in the content of polyunsaturated fatty acids in the membranes of the two cell types. RAW264.7 cells contain high concentrations of 18:1, which might, in part, substitute for the longer chain, more highly unsaturated fatty acids found in RPM. The high 18:1 content is retained in 20:4-enriched RAW264.7 cells, contributing to the differences in species distribution among glycerophospholipids between these cells and RPM. For example,

20:4 enrichment leads to significant increases in 38:5 GPCho and GPIs, leading to much higher levels of these lipids than are seen in RPM. Despite the elevation in 18:1, it is likely that the relative deficit in 20:4 and other polyunsaturated fatty acids in RAW264.7 cells leads to a corresponding deficit in membrane fluidity as compared to RPM. This would be expected to lead to impairment of basic functions such as pinocytosis and phagocytosis in the RAW264.7 cell (27,28).

In the past 20 years, it has become increasingly evident that glycerophospholipid metabolism plays a central role in multiple aspects of cellular physiology, including stimulus-response coupling, lipid mediator biosynthesis, membrane trafficking and fusion, and membrane-bound protein function, emphasizing the need for a comprehensive evaluation of the glycerophospholipid metabolome. In the past, lipid metabolic studies have emphasized the precise substrate-product relationships of individual enzymes, such as phospholipase C (PLC) and cPLA<sub>2</sub> (among others) that respond to a stimulus such as LPS. Although this is a desirable goal, it is equally important to characterize the overall physiological consequences of cell surface receptor activation and the subsequent metabolic responses. The mass spectrometry-based lipid analysis shown in this work represents the end result of the integrated steady-state activities of all of the lipid metabolic enzymes in resting macrophages (for control cells) or the sum total of all of the lipolytic and lipid synthetic activities that occur as a result of stimulation (in LPS-treated cells). The enzymatic activities that regulate the lipid metabolome of intact cells have yet to be comprehensively identified, but as demonstrated here, the sum of the glycerophospholipid changes resulting from a specific environmental challenge can now be systematically evaluated. In this way we are able to assess the glycerophospholipid status of selected cell populations prior to stimulation, and to define the integrated receptor-mediated changes in cell membrane composition for any stimulation paradigm. This detailed analysis is essential to understanding the sequence of cell signaling and lipid metabolic events initiated by any stimulus that leads to glycerophospholipid turnover. The present work illustrates only a small fraction of the information that can be gleaned by this approach, yet it clearly demonstrates the importance of the comprehensive evaluation of glycerophospholipid composition and structure in the interpretation of cellular physiological responses.

## SUPPORTING INFORMATION AVAILABLE

Refer to Web version on PubMed Central for supplementary material.

## Acknowledgements

The authors thank Andrew Goodman and Michelle Armstrong for excellent technical assistance.

## References

1. Gijon MA, Leslie CC. Regulation of arachidonic acid release and cytosolic phospholipase A2 activation. *J Leukoc Biol* 1999;65:330–336. [PubMed: 10080535]
2. Gijon MA, Spencer DM, Siddiqi AR, Bonventre JV, Leslie CC. Cytosolic phospholipase A2 is required for macrophage arachidonic acid release by agonists that Do and Do not mobilize calcium. Novel role of mitogen-activated protein kinase pathways in cytosolic phospholipase A2 regulation. *J Biol Chem* 2000;275:20146–20156. [PubMed: 10867029]
3. Hirabayashi T, Shimizu T. Localization and regulation of cytosolic phospholipase A(2). *Biochim Biophys Acta* 2000;1488:124–138. [PubMed: 11080682]
4. Fujishima H, Sanchez Mejia RO, Bingham CO 3rd, Lam BK, Sapirstein A, Bonventre JV, Austen KF, Arm JP. Cytosolic phospholipase A2 is essential for both the immediate and the delayed phases of eicosanoid generation in mouse bone marrow-derived mast cells. *Proc Natl Acad Sci USA* 1999;96:4803–7. [PubMed: 10220374]



5. Samuelsson B, Dahlen SE, Lindgren JA, Rouzer CA, Serhan CN. Leukotrienes and lipoxins: structures, biosynthesis, and biological effects. *Science* 1987;237:1171–1176. [PubMed: 2820055]
6. Samuelsson B, Goldyne M, Granstrom E, Hamberg M, Hammarstrom S, Malmsten C. Prostaglandins and thromboxanes. *Ann Rev Biochem* 1978;47:997–1029. [PubMed: 209733]
7. Pace-Asciak CR, Asotra S. Biosynthesis, catabolism, and biological properties of HPETEs, hydroperoxide derivatives of arachidonic acid. *Free Radic Biol Med* 1989;7:409–433. [PubMed: 2514125]
8. Snyder F. Metabolism of platelet activating factor and related ether lipids: enzymatic pathways, subcellular sites, regulation, and membrane processing. *Prog Clin Biol Res* 1988;282:57–72. [PubMed: 3071807]
9. Hillard CJ. Biochemistry and pharmacology of the endocannabinoids arachidonylethanolamide and 2-arachidonylglycerol. *Prostaglandins Other Lipid Mediat* 2000;61:3–18. [PubMed: 10785538]
10. Scott WA, Zrike JM, Hamill AL, Kempe J, Cohn ZA. Regulation of arachidonic acid metabolites in macrophages. *J Exp Med* 1980;152:324–335. [PubMed: 7400759]
11. Mason RJ, Stossel TP, Vaughan M. Lipids of alveolar macrophages, polymorphonuclear leukocytes, and their phagocytic vesicles. *J Clin Invest* 1972;51:2399–2407. [PubMed: 4344731]
12. Humes JL, Bonney RJ, Pelus L, Dahlgren ME, Sadowski SJ, Kuehl FA Jr, Davies P. Macrophages synthesis and release prostaglandins in response to inflammatory stimuli. *Nature* 1977;269:149–151. [PubMed: 561892]
13. Rouzer CA, Scott WA, Kempe J, Cohn ZA. Prostaglandin synthesis by macrophages requires a specific receptor-ligand interaction. *Proc Natl Acad Sci USA* 1980;77:4279–4282. [PubMed: 6933478]
14. Rouzer CA, Scott WA, Hamill AL, Liu FT, Katz DH, Cohn ZA. IgE immune complexes stimulate arachidonic acid release by mouse peritoneal macrophages. *Proc Natl Acad Sci USA* 1982;79:5656–5660. [PubMed: 6813864]
15. Abiko Y, Shibata Y, Fukushima K, Murai S, Takiguchi H. The stimulation of macrophage prostaglandin E2 and thromboxane B2 secretion by *Streptococcus mutans* insoluble glucans. *FEBS Lett* 1983;154:297–300. [PubMed: 6403385]
16. Chang J, Wigley F, Newcombe D. Neutral protease activation of peritoneal macrophage prostaglandin synthesis. *Proc Natl Acad Sci USA* 1980;77:4736–4740. [PubMed: 7001465]
17. Dentan C, Lesnik P, Chapman MJ, Ninio E. Phagocytic activation induces formation of platelet-activating factor in human monocyte-derived macrophages and in macrophage-derived foam cells. Relevance to the inflammatory reaction in atherogenesis. *Eur J Biochem* 1996;236:48–55. [PubMed: 8617285]
18. Elstad MR, Stafforini DM, McIntyre TM, Prescott SM, Zimmerman GA. Platelet-activating factor acetylhydrolase increases during macrophage differentiation. A novel mechanism that regulates accumulation of platelet-activating factor. *J Biol Chem* 1989;264:8467–8470. [PubMed: 2722780]
19. Ivanova PT, Cerda BA, Horn DM, Cohen JS, McLafferty FW, Brown HA. Electrospray ionization mass spectrometry analysis of changes in phospholipids in RBL-2H3 mastocytoma cells during degranulation. *Proc Natl Acad Sci U S A* 2001;98:7152–7157. [PubMed: 11416200]
20. Forrester JS, Milne SB, Ivanova PT, Brown HA. Computational lipidomics: a multiplexed analysis of dynamic changes in membrane lipid composition during signal transduction. *Mol Pharmacol* 2004;65:813–821. [PubMed: 15044609]
21. Raschke WC, Baird S, Ralph P, Nakoinz I. Functional macrophage cell lines transformed by Abelson leukemia virus. *Cell* 1978;15:261–267. [PubMed: 212198]
22. Hwang D, Jang BC, Yu G, Boudreau M. Expression of mitogen-inducible cyclooxygenase induced by lipopolysaccharide: mediation through both mitogen-activated protein kinase and NF-kappaB signaling pathways in macrophages. *Biochem Pharmacol* 1997;54:87–96. [PubMed: 9296354]
23. Lo CJ, Cryer HG, Fu M, Lo FR. Regulation of macrophage eicosanoid generation is dependent on nuclear factor kappaB. *J Trauma* 1998;45:19–24. [PubMed: 9680006]
24. Giroux M, Descoteaux A. Cyclooxygenase-2 expression in macrophages: modulation by protein kinase C-alpha. *J Immunol* 2000;165:3985–3991. [PubMed: 11034408]

25. Hsu YW, Chi KH, Huang WC, Lin WW. Ceramide inhibits lipopolysaccharide-mediated nitric oxide synthase and cyclooxygenase-2 induction in macrophages: effects on protein kinases and transcription factors. *J Immunol* 2001;166:5388–5397. [PubMed: 11313375]
26. Wadleigh DJ, Reddy ST, Kopp E, Ghosh S, Herschman HR. Transcriptional activation of the cyclooxygenase-2 gene in endotoxin-treated RAW 264.7 macrophages. *J Biol Chem* 2000;275:6259–6266. [PubMed: 10692422]
27. Mahoney EM, Hamill AL, Scott WA, Cohn ZA. Response of endocytosis to altered fatty acyl composition of macrophage phospholipids. *Proc Natl Acad Sci U S A* 1977;74:4895–4899. [PubMed: 270722]
28. Mahoney EM, Scott WA, Landsberger FR, Hamill AL, Cohn ZA. Influence of fatty acyl substitution on the composition and function of macrophage membranes. *J Biol Chem* 1980;255:4910–4917. [PubMed: 6246087]
29. Rouzer CA, Marnett LJ. Glycerylprostaglandin synthesis by resident peritoneal macrophages in response to a zymosan stimulus. *J Biol Chem* 2005;280:26690–700. [PubMed: 15917246]
30. Kingsley PJ, Rouzer CA, Saleh S, Marnett LJ. Simultaneous analysis of prostaglandin glyceryl esters and prostaglandins by electrospray tandem mass spectrometry. *Anal Biochem* 2005;343:203–211. [PubMed: 16004953]
31. Zhu MY, Hasty AH, Harris C, Linton MF, Fazio S, Swift LL. Physiological relevance of apolipoprotein E recycling: studies in primary mouse hepatocytes. *Metabolism* 2005;54:1309–1315. [PubMed: 16154429]
32. Milne, SB.; Forrester, JS.; Ivanova, PT.; Armstrong, MD.; Brown, HA. AfCs Research Report. 2003. pp [www.signaling-gateway.org/reports/v1/DA0011/DA0011.htm](http://www.signaling-gateway.org/reports/v1/DA0011/DA0011.htm).
33. Milne S, Ivanova P, Forrester J, Brown HA. Lipidomics: An analysis of cellular lipids by ESI-MS. *Methods* 2006;39:92–103. [PubMed: 16846739]
34. Rouzer CA, Kingsley PJ, Wang H, Zhang H, Morrow JD, Dey SK, Marnett LJ. Cyclooxygenase-1-dependent prostaglandin synthesis modulates tumor necrosis factor- $\alpha$  secretion in lipopolysaccharide-challenged murine resident peritoneal macrophages. *J Biol Chem* 2004;279:34256–34268. [PubMed: 15181007]
35. Murphy, RC. Mass spectrometry of phospholipids: tables of molecular and product ions. Illuminati Press; Denver, CO: 2002.
36. Brugger B, Erben G, Sandhoff R, Wieland FT, Lehmann WD. Quantitative analysis of biological membrane lipids at the low picomole level by nano-electrospray ionization tandem mass spectrometry. *Proc Natl Acad Sci U S A* 1997;94:2339–2344. [PubMed: 9122196]
37. Gaposchkin DP, Zoeller RA. Plasmalogen status influences docosahexaenoic acid levels in a macrophage cell line. Insights using ether lipid-deficient variants. *J Lipid Res* 1999;40:495–503. [PubMed: 10064738]
38. Scott WA, Pawlowski NA, Murray HW, Andreach M, Zrike J, Cohn ZA. Regulation of arachidonic acid metabolism by macrophage activation. *J Exp Med* 1982;155:1148–1160. [PubMed: 6801185]
39. Rouzer CA, Jacobs AT, Nirodi CS, Kingsley PJ, Morrow JD, Marnett LJ. RAW264.7 cells lack prostaglandin-dependent autoregulation of tumor necrosis factor- $\alpha$  secretion. *J Lipid Res* 2005;46:1027–1037. [PubMed: 15722559]
40. Lendemans S, Rani M, Selbach C, Kreuzfelder E, Schade FU, Flohe S. GM-CSF priming of human monocytes is dependent on ERK1/2 activation. *J Endotoxin Res* 2006;12:10–20. [PubMed: 16420740]
41. Arias-Negrete S, Keller K, Chadee K. Proinflammatory cytokines regulate cyclooxygenase-2 mRNA expression in human macrophages. *Biochem Biophys Res Commun* 1995;208:582–589. [PubMed: 7695610]
42. Perkins DJ, Kniss DA. Blockade of nitric oxide formation down-regulates cyclooxygenase-2 and decreases PGE2 biosynthesis in macrophages. *J Leukoc Biol* 1999;65:792–799. [PubMed: 10380901]
43. Nakagawa Y, Ishii E. Changes in arachidonic acid metabolism and the aggregation of polymorphonuclear leukocytes in rats with streptozotocin-induced diabetes. *Biochim Biophys Acta* 1996;1315:145–151. [PubMed: 8608172]

44. Chilton FH, Connell TR. 1-ether-linked phosphoglycerides. Major endogenous sources of arachidonate in the human neutrophil. *J Biol Chem* 1988;263:5260–5265. [PubMed: 3128538]
45. Nakagawa Y, Kurihara K, Sugiura T, Waku K. Relative degradation of different arachidonoyl molecular species of choline glycerophospholipids in opsonized zymosan-stimulated rabbit alveolar macrophages. *Biochim Biophys Acta* 1986;876:601–610. [PubMed: 3085723]

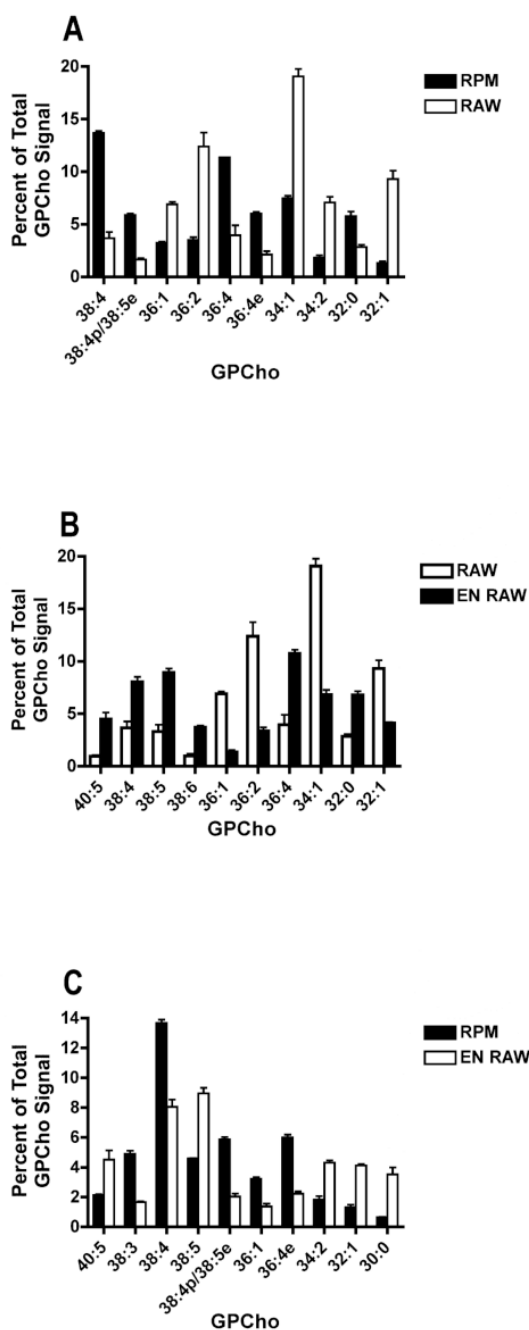
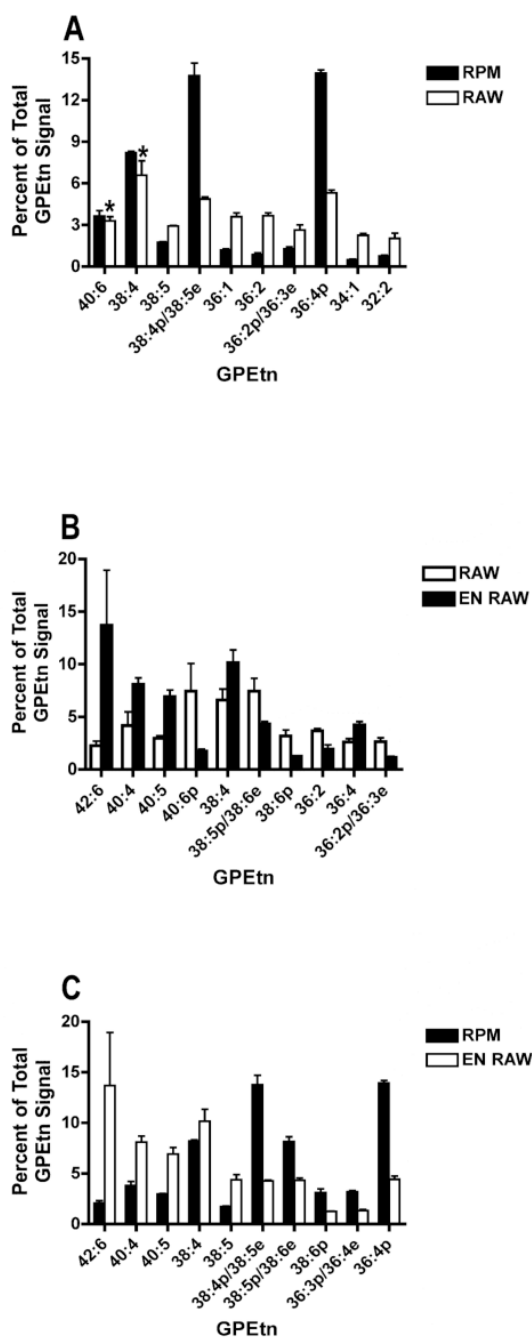


**Figure 1.**

Comparison of relative distribution of individual GPCho species in RAW264.7 cells 20:4-enriched RAW264.7 cells, and RPM. RAW264.7 cells (60 mm dishes) were preincubated for 22 h with 20 ng/ml GM-CSF in DMEM/FCS (RAW) or with 20 ng/ml GM-CSF in SFM-20:4 (EN RAW). RPM were isolated and incubated overnight in  $\alpha$ -MEM/FCS. The cells were harvested for analysis of total glycerophospholipids by MS. The total signal intensities of 31 distinct GPCho species were summed, and the magnitude of the signal intensity of each species was then calculated as a percent of that total. *A* The 10 species that showed the greatest differences between RAW264.7 cells and RPM are shown. *B* The 10 species that showed the greatest differences between RAW264.7 cells and 20:4-enriched RAW264.7 cells are shown.

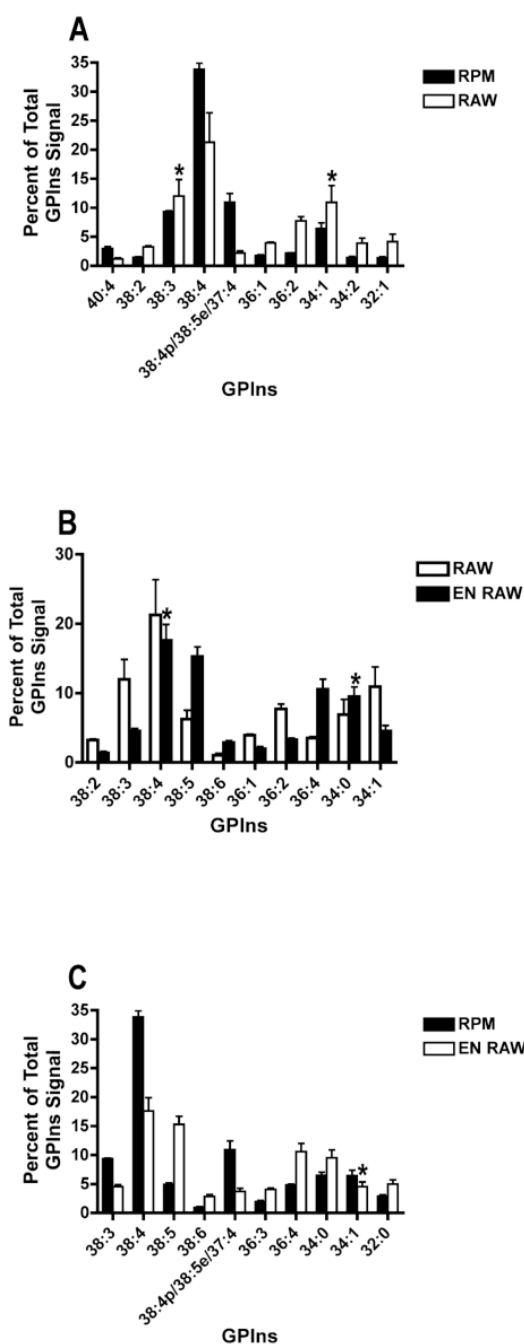
C The 10 species that showed the greatest differences between 20:4-enriched RAW264.7 cells and RPM are shown. Results are the mean  $\pm$  standard deviation of the combined results from three separate experiments in which triplicate determinations were made. The comparative differences between cell types were statistically significant ( $p < 0.05$ ) for all species unless designated by an asterisk. Data for all 31 GPCho species are given in Fig. S3 in Supplemental Material.





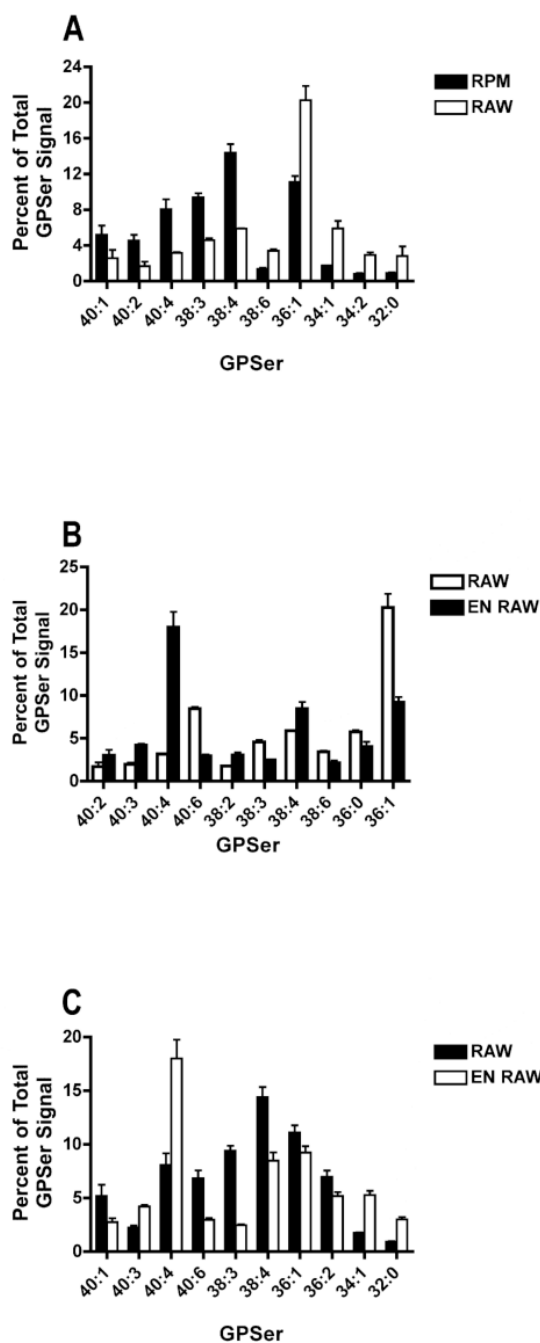
**Figure 2.**

Comparison of relative distribution of individual GPEtn species in RAW264.7 cells, 20:4-enriched RAW264.7 cells and RPM. Conditions are identical to those described in the legend to Fig. 3, except that data are given for GPEtn (38 distinct species analyzed). Data for all 38 GPEtn species are given in Fig. S4 in Supplemental Material.



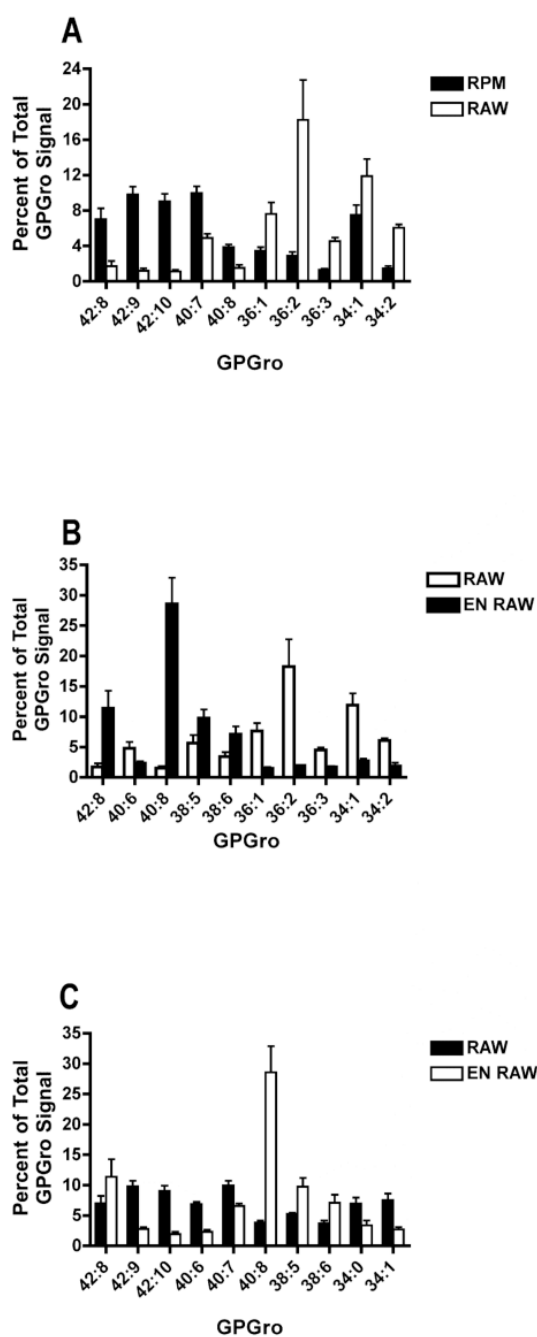
**Figure 3.**

Comparison of relative distribution of individual GPIs species in RAW264.7 cells, 20:4-enriched RAW264.7 cells and RPM. Conditions are identical to those described in the legend to Fig. 3, except that data are given for GPIs (20 distinct species analyzed). Data for all 20 GPIs species are given in Fig. S5 in Supplemental Material.



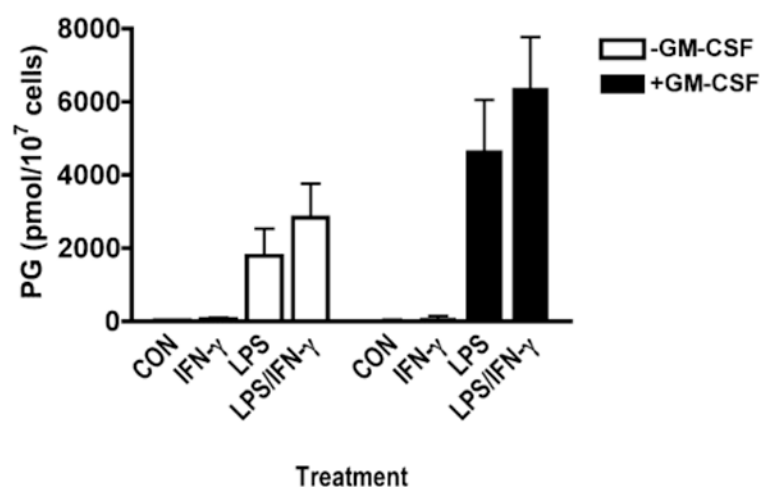
**Figure 4.**

Comparison of relative distribution of individual GPSer species in RAW264.7 cells, 20:4-enriched RAW264.7 cells and RPM. Conditions are identical to those described in the legend to Fig. 3, except that data are given for GPSer (23 distinct species analyzed). Data for all 23 GPSer species are given in Fig. S6 in Supplemental Material.



**Figure 5.**

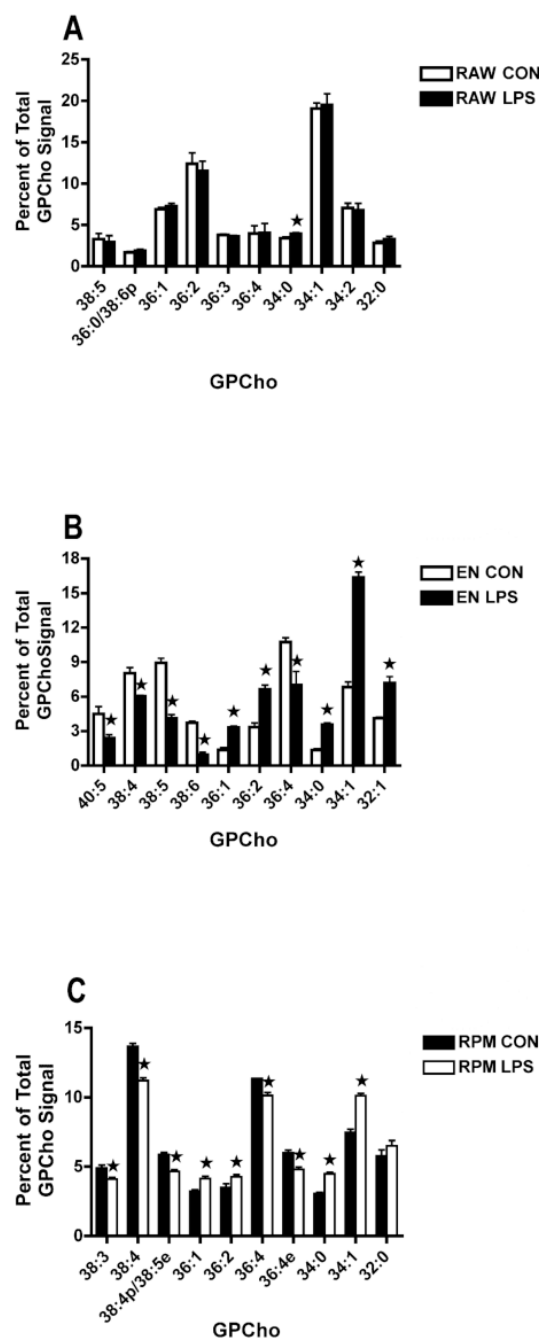
Comparison of relative distribution of individual GPGro species in RAW264.7 cells, 20:4-enriched RAW264.7 cells and RPM. Conditions are identical to those described in the legend to Fig. 3, except that data are given for GPGro (25 distinct species analyzed). Data for all 25 GPGro species are given in Fig. S7 in Supplemental Material.



**Figure 6.**

Effect of GM-CSF, LPS, and IFN- $\gamma$  on PG synthesis in RAW264.7 cells. A RAW264.7 cells (35 mm dishes) were preincubated for 22 h in the presence (+GM-CSF) or absence (-GM-CSF) of 20 ng/ml of GM-CSF. The cells were then transferred to fresh DMEM/FCS containing no additional stimulus (CON), 10 ng/ml IFN- $\gamma$  (IFN- $\gamma$ ), 100 ng/ml LPS (LPS), or LPS plus IFN- $\gamma$  (LPS/IFN- $\gamma$ ). The medium also contained GM-CSF in the case of cells preincubated with that cytokine. Following a 6 h incubation, the medium was harvested and analyzed for PGs by LC-MS/MS. All data are the mean  $\pm$  standard deviation from three separate experiments in which triplicate determinations were made.

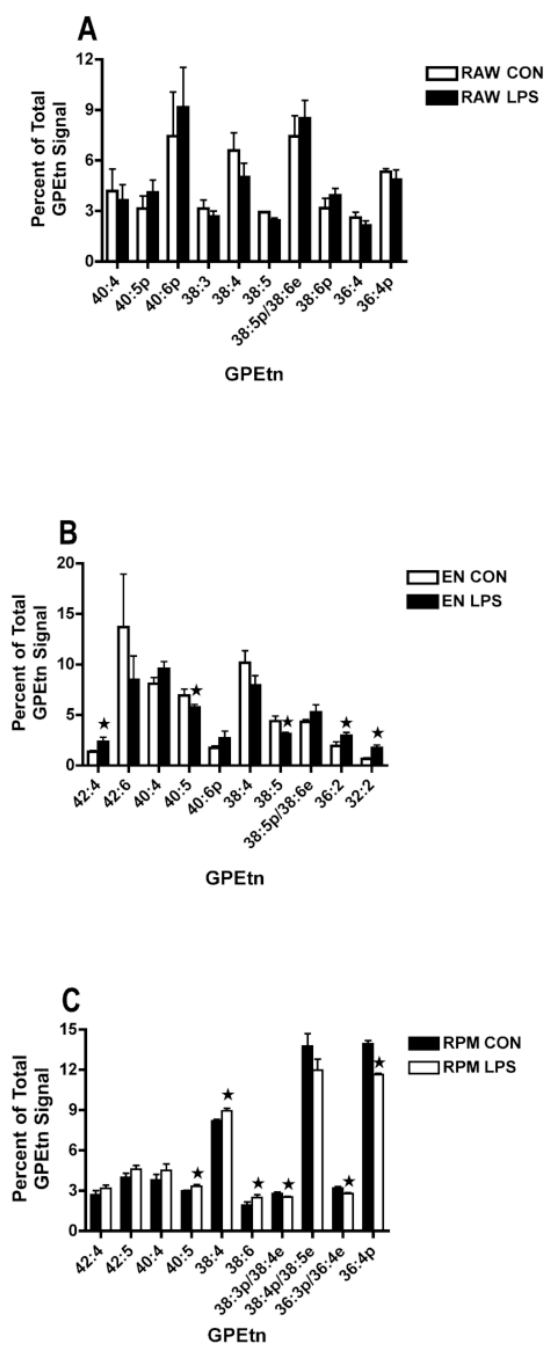




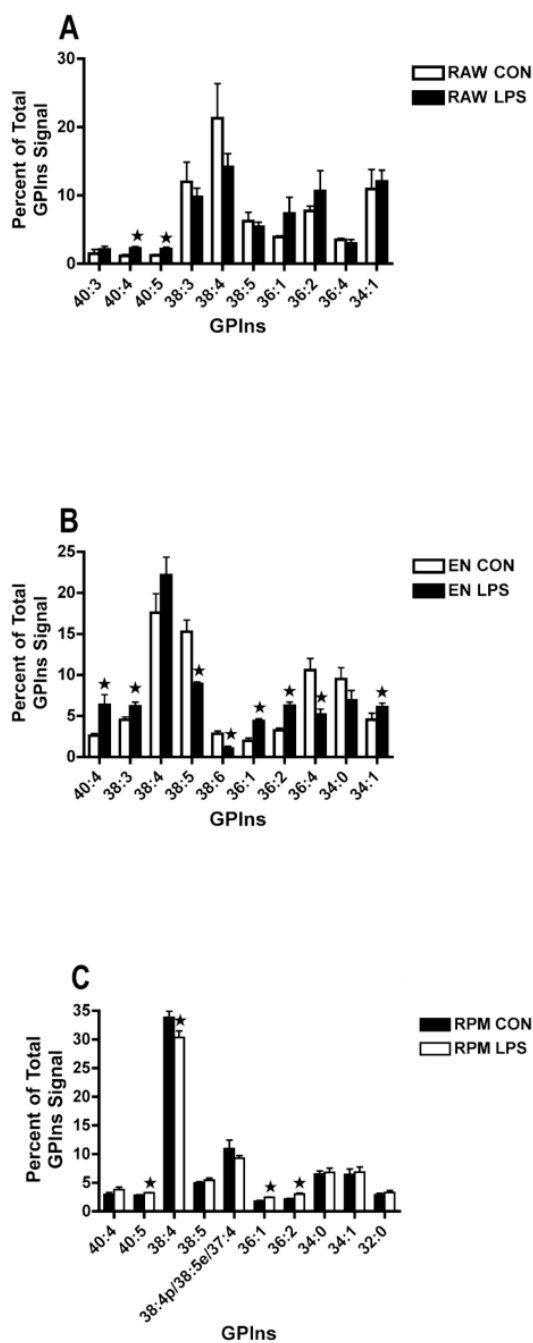
**Figure 7.**

Effect of LPS treatment on the relative distribution of GPCho species. **A** RAW264.7 cells (60 mm dishes) were preincubated for 22 h with 20 ng/ml GM-CSF in DMEM/FCS. Cells were then transferred to fresh DMEM/FCS containing GM-CSF plus 10 ng/mL IFN- $\gamma$  and 100 ng/ml LPS and incubated for an additional 5 h. Data show a comparison for cells harvested immediately at the end of the 22 h GM-CSF preincubation (RAW CON) and cells subjected to the 5 h treatment with LPS/IFN- $\gamma$  (RAW LPS). **B** RAW264.7 cells (60 mm dishes) were preincubated for 22 h with 20 ng/ml GM-CSF in SFM-20:4. Cells were then transferred to fresh DMEM/FCS containing GM-CSF plus 10 ng/mL IFN- $\gamma$  and 100 ng/ml LPS and incubated for an additional 5 h. Data show a comparison of cells harvested immediately at the end of the

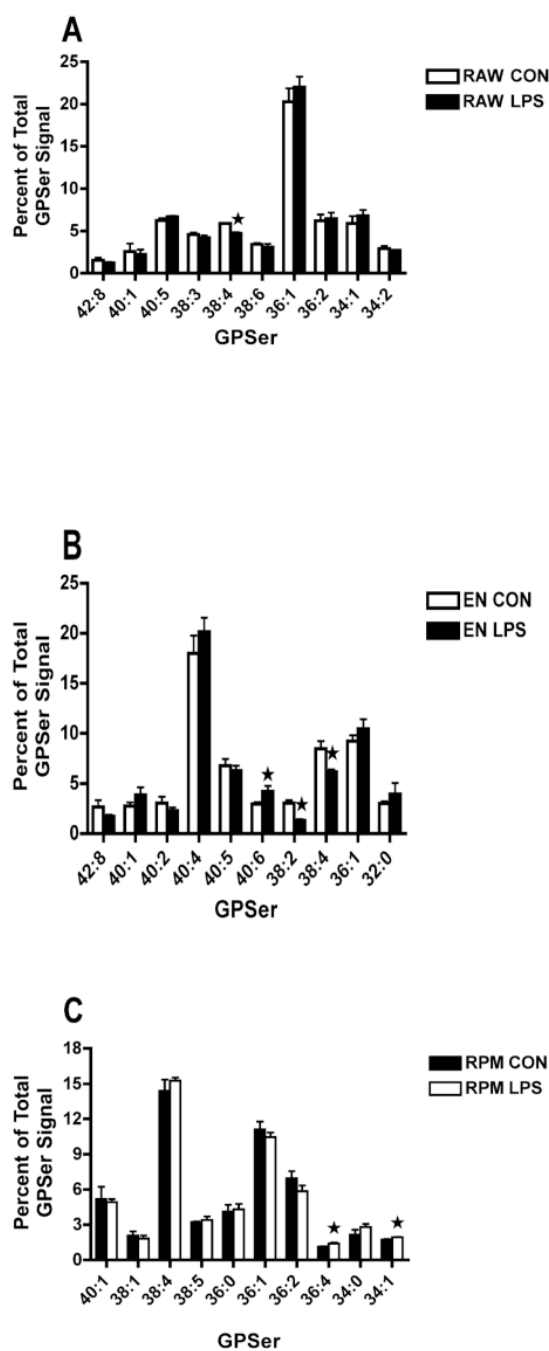
22 h GM-CSF preincubation (EN CON) and cells subjected to the 5 h treatment with LPS/IFN- $\gamma$  (EN LPS). C RPM (60 mm dishes) were isolated and incubated overnight in  $\alpha$ -MEM/FCS. Cells were then transferred to fresh  $\alpha$ -MEM/FCS containing 100 ng/ml LPS and incubated for an additional 5 h. Data show a comparison of cells harvested immediately at the end of the overnight incubation (RPM CON) and cells subjected to the 5 h treatment with LPS (RPM LPS). In all cases, cells were harvested for analysis of total phospholipids by MS. The signal intensities from 31 distinct GPCho species were summed, and the magnitude of the signal intensity of each species was then calculated as a percent of that total. The 10 species demonstrating the greatest differences between the two cell populations are shown here. Results are the mean  $\pm$  standard deviation of the combined results from three separate experiments in which triplicate determinations were made. Species designated with a star were statistically significant ( $p < 0.05$ ). Data for all 31 GPCho species are given in Fig. S8 in Supplemental Material.

**Figure 8.**

Effect of LPS treatment on the relative distribution of GPEtn species. Conditions are identical to those described in the legend to Fig. 8, except that data are given for GPEtn (38 distinct species analyzed). Data for all 38 GPEtn species are given in Fig. S9 in Supplemental Material.

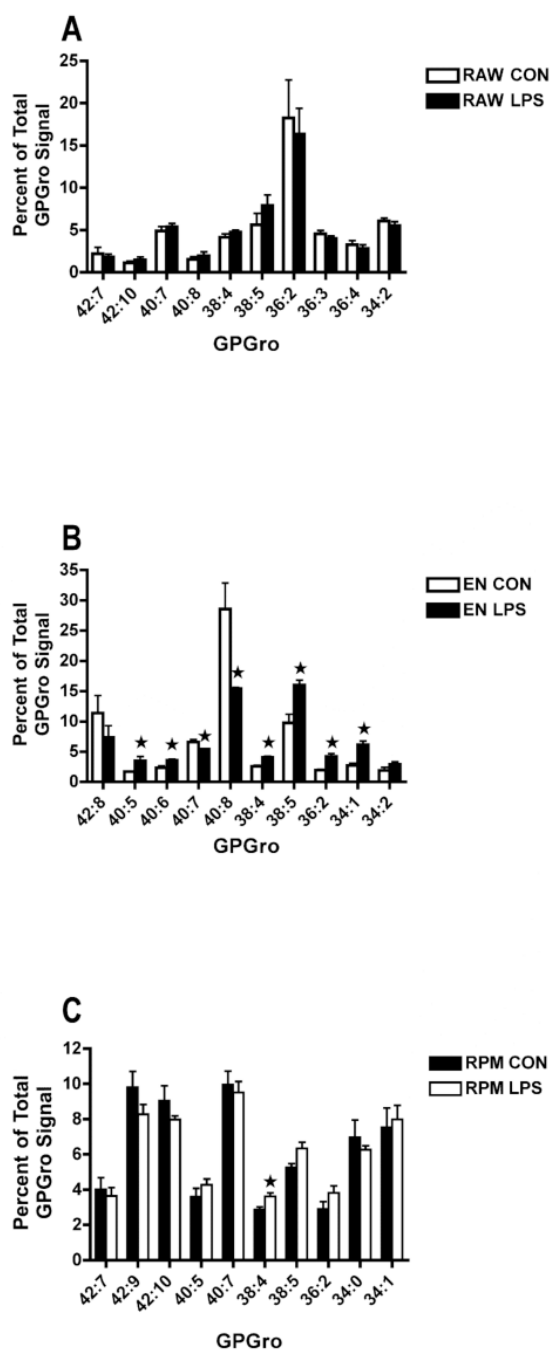
**Figure 9.**

Effect of LPS treatment on the relative distribution of GPIs species. Conditions are identical to those described in the legend to Fig. 8, except that data are given for GPIs (20 distinct species analyzed). Data for all 20 GPIs species are given in Fig. S10 in Supplemental Material.

**Figure 10.**

Effect of LPS treatment on the relative distribution of GPSer species. Conditions are identical to those described in the legend to Fig. 8, except that data are given for GPSer (23 distinct species analyzed). Data for all 23 GPSer species are given in Fig. S11 in Supplemental Material.



**Figure 11.**

Effect of LPS treatment on the relative distribution of GPGro species. Conditions are identical to those described in the legend to Fig. 8, except that data are given for GPGro (25 distinct species analyzed). Data for all 25 GPGro species are given in Fig. S12 in Supplemental Material.

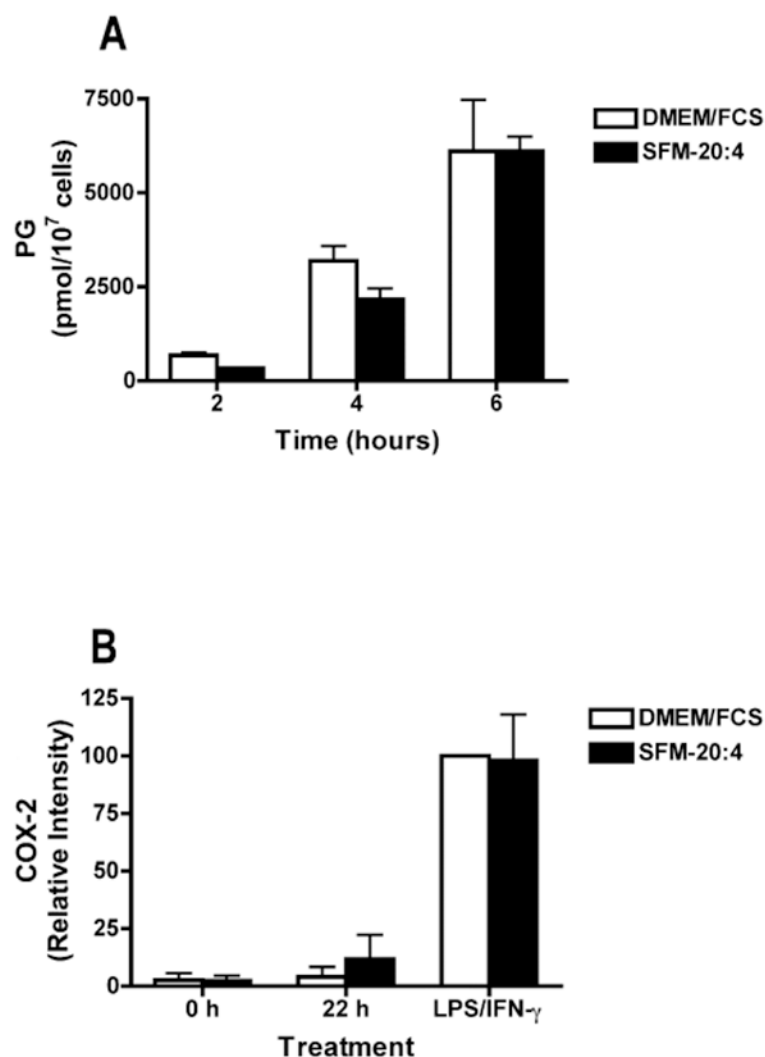


**Figure 12.**

Effect of 20:4 enrichment on PG synthesis and COX-2 expression. RAW264.7 cells (35 mm dishes) were preincubated for 22 h with GM-CSF in DMEM/FCS or SFM-20:4 as indicated. The cells were then transferred to DMEM/FCS containing GM-CSF, LPS and IFN- $\gamma$ . **A** At the indicated times, the medium was harvested for analysis of PG formation from endogenous substrate by LC-MS/MS. **B** The cells were harvested at the beginning of the GM-CSF pretreatment period (0 h), at the end of that period (22 h) and at the end of the treatment with LPS and IFN- $\gamma$  (LPS/IFN- $\gamma$ ) for immunoblot analysis for expression of COX-2. Chemiluminescence was measured by a Fluor-S Max Multi-Imager, and the data were normalized to the signal obtained in cells pretreated with GM-CSF in DMEM/FCS and incubated with LPS and IFN- $\gamma$ . The results are the mean  $\pm$  standard deviation from three separate experiments in which triplicate determinations were made.

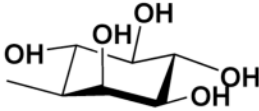
**Table 1**  
Phospholipid fatty acid composition of RAW264.7 cells and RPM.

Fatty Acid	Fatty Acid Composition (mole percent)					
	RPM		RAW264.7 Control			RAW264.7 Enriched
	CON	LPS	CON	LPS/INF- $\gamma$	CON	LPS/INF- $\gamma$
14:0	0.0 $\pm$ 0.0	0.0 $\pm$ 0.0	0.8 $\pm$ 0.9	0.9 $\pm$ 0.6	2.7 $\pm$ 0.8	2.7 $\pm$ 0.1
16:0	24 $\pm$ 1	26 $\pm$ 1	24 $\pm$ 1	26 $\pm$ 1	23 $\pm$ 4.8	30 $\pm$ 1
16:1	0.0 $\pm$ 0.0	0.0 $\pm$ 0.0	4.5 $\pm$ 0.5	5.1 $\pm$ 0.4	4.4 $\pm$ 3.5	3.8 $\pm$ 0.1
18:0	22 $\pm$ 1	23 $\pm$ 1	18 $\pm$ 2	18 $\pm$ 1	9.5 $\pm$ 1.3	14 $\pm$ 1
18:1	7.8 $\pm$ 0.3	9.5 $\pm$ 0.1	32 $\pm$ 1	33 $\pm$ 1	15 $\pm$ 2	22 $\pm$ 1
18:2	4.0 $\pm$ 0.2	3.3 $\pm$ 0.1	3.0 $\pm$ 0.2	3.1 $\pm$ 0.1	6.8 $\pm$ 1.2	3.8 $\pm$ 0.1
20:3 $\omega$ 9	0.0 $\pm$ 0.0	0.0 $\pm$ 0.0	3.0 $\pm$ 0.1	2.3 $\pm$ 0.1	0.6 $\pm$ 1.0	0.0 $\pm$ 0.0
20:3 $\omega$ 6	3.7 $\pm$ 0.3	3.6 $\pm$ 0.3	0.5 $\pm$ 0.8	1.0 $\pm$ 0.2	0.4 $\pm$ 0.7	0.6 $\pm$ 0.5
20:3 $\omega$ 3	0.0 $\pm$ 0.0	0.0 $\pm$ 0.0	0.0 $\pm$ 0.0	0.0 $\pm$ 0.0	0.9 $\pm$ 1.5	0.0 $\pm$ 0.0
20:4	26 $\pm$ 1	23 $\pm$ 1	10 $\pm$ 1	7.4 $\pm$ 1.2	20 $\pm$ 1	12 $\pm$ 1
20:5	0.0 $\pm$ 0.0	0.0 $\pm$ 0.0	0.0 $\pm$ 0.0	0.0 $\pm$ 0.0	2.0 $\pm$ 3.5	0.0 $\pm$ 0.0
22:4	4.4 $\pm$ 0.7	4.9 $\pm$ 1.0	0.5 $\pm$ 0.4	0.1 $\pm$ 0.2	13 $\pm$ 3	12 $\pm$ 1
22:5	3.0 $\pm$ 0.3	3.0 $\pm$ 0.2	1.7 $\pm$ 0.3	1.8 $\pm$ 0.3	1.5 $\pm$ 2.5	0.2 $\pm$ 0.4
22:6	4.4 $\pm$ 0.7	3.9 $\pm$ 0.6	1.7 $\pm$ 0.2	1.8 $\pm$ 0.2	0.0 $\pm$ 0.0	0.0 $\pm$ 0.0

RAW264.7 cells (60 mm dishes) were preincubated for 22 h with 20 ng/ml GM-CSF in DMEM/FCS (Control) or SFM-20:4 (Enriched). RPM were isolated and incubated for 22 h in  $\alpha$ -MEM. Cells were then transferred to DMEM/FCS plus 20 ng/ml GM-CSF, 10 ng/ml INF- $\gamma$  and 100 ng/ml LPS (for RAW264.7 cells) or to  $\alpha$ -MEM plus 100 ng/ml LPS (for RPM). Cells were incubated for an additional 5 h. The cells were harvested for fatty acid analysis either at the end of the 22 h incubation (CON) or at the end of the 5 h incubation (LPS). Results are expressed as mole percent for each fatty acid, and are the mean  $\pm$  standard deviation of the combined results from three separate experiments in which triplicate determinations were made.

Table 2

Phospholipid structures and nomenclature.

<div>38:4</div> <div>38:4e</div> <div>38:4p</div>				
X=	Structure	Class	Structure	Class
	$\text{-CH}_2\text{CH}_2\text{N}^+(\text{CH}_3)_3$	GPCho	$\text{-CH}_2\text{CH}(\text{OH})\text{CH}_2\text{OH}$	GPGro
	$\text{-CH}_2\text{CH}_2\text{NH}_2$	GPEtn		GPIns
	$\text{-CH}_2\text{CH}(\text{COOH})\text{NH}_2$	GPSer		

General structure of a 38:4 phospholipid. In this case, the fatty acids are 18:0 and 20:4. Other combinations of fatty acids having a total of 38 carbons and 4 double bonds can yield the 38:4 designation as shown in Table 1 (Supplement). Lipids designated “e” and “p” have ether and vinyl ether linkages at the *sn-1* position, respectively. The -X moiety represents the headgroup shown below the structures. The headgroup specifies the lipid class.

**Table 3**

Percent signal intensity and estimated absolute quantities of 20:4-containing lipids in glycerophospholipid classes.

Lipid Class	20:4-Containing Lipids		
	Percent Signal Intensity (nmol/10 <sup>7</sup> cells)		
	RPM	RAW264.7 Control	RAW264.7 Enriched
GPCho	48 ± 1 (48 ± 1)	19 ± 3 (17 ± 3)	41 ± 1 (35 ± 1)
GPEtn	63 ± 1 (44 ± 1)	43 ± 1 (18 ± 1)	59 ± 2 (24 ± 1)
GPIns	57 ± 2 (7.1 ± 0.3)	32 ± 5 (4.2 ± 0.6)	51 ± 4 (6.1 ± 0.5)
GPSer	23 ± 1 (3.1 ± 0.1)	19 ± 1 (2.5 ± 0.1)	20 ± 1 (2.6 ± 0.2)
GPGro	47 ± 4 (6.7 ± 0.5)	21 ± 5 (2.7 ± 0.6)	68 ± 4 (8.6 ± 0.5)

RAW264.7 cells (60 mm dishes) were preincubated for 22 h with 20 ng/ml GM-CSF in DMEM/FCS (Control) or SFM-20:4 (Enriched). RPM were isolated and incubated for 22 h in  $\alpha$ -MEM/FCS. The cells were harvested for total glycerophospholipid analysis. Results are the sum of the percent of the total signal intensity of all peaks in a lipid class that contain 20:4, and are the mean  $\pm$  standard deviation of the combined results from three independent experiments in which triplicate determinations were made. Values in parentheses were derived by using the percent signal intensity to calculate an estimated absolute amount of each lipid (in nmol/10<sup>7</sup> cells), using published quantities of each lipid class in RPM (28) and RAW264.7 cells (37).

**Table 4**Effects of LPS/IFN- $\gamma$  treatment on RAW264.7 cell and RPM 20:4 content.

Cell Type	Treatment	20:4 (nmol/10 <sup>7</sup> cells)	$\Delta$ 20:4 from CON (PGs formed) (nmol/10 <sup>7</sup> cells)
RPM	CON	110 $\pm$ 4	NA
RPM	LPS	100 $\pm$ 6	10 $\pm$ 3
RAW	CON	38 $\pm$ 5	(6.9 $\pm$ 1.4) *
RAW	LPS/IFN- $\gamma$	27 $\pm$ 4	NA
EN-RAW	CON	76 $\pm$ 4	11 $\pm$ 3
EN-RAW	LPS/IFN- $\gamma$	43 $\pm$ 1	(6.4 $\pm$ 1.4) *
			NA
			33 $\pm$ 6
			(6.1 $\pm$ 0.4) *

Experimental conditions are as described in the legend to Table 1, and the data are derived from Table 1. Values for the mole percent of 20:4 under the various experimental conditions were converted to an estimated absolute value for 20:4 content in the cells as described in Experimental Procedures. For each set of experimental conditions the loss of 20:4 during treatment with LPS/IFN- $\gamma$  (RAW264.7 cells) or LPS alone (RPM) was calculated.

\* Data are from (34, Fig. 6 and Fig. 12).